



HAL
open science

Structure and photoluminescence properties of evaporated GeOx thin films

M. Ardyanian, Hervé Rinnert, X. Devaux, M. Vergnat

► **To cite this version:**

M. Ardyanian, Hervé Rinnert, X. Devaux, M. Vergnat. Structure and photoluminescence properties of evaporated GeOx thin films. Applied Physics Letters, 2006, 89, pp.011902. 10.1063/1.2218830 . hal-02164231

HAL Id: hal-02164231

<https://hal.science/hal-02164231>

Submitted on 24 Jun 2019

HAL is a multi-disciplinary open access archive for the deposit and dissemination of scientific research documents, whether they are published or not. The documents may come from teaching and research institutions in France or abroad, or from public or private research centers.

L'archive ouverte pluridisciplinaire **HAL**, est destinée au dépôt et à la diffusion de documents scientifiques de niveau recherche, publiés ou non, émanant des établissements d'enseignement et de recherche français ou étrangers, des laboratoires publics ou privés.

Structure and photoluminescence properties of evaporated GeO_x thin films

M. Ardyanian, H. Rinnert, X. Devaux, and M. Vergnat^{a)}

Laboratoire de Physique des Matériaux (UMR CNRS No. 7556), Université de Nancy 1, Boîte Postale 239, 54506 Vandœuvre-lès-Nancy Cedex, France

(Received 27 February 2006; accepted 16 May 2006; published online 5 July 2006)

Amorphous GeO_x alloys were prepared by evaporation of GeO_2 powder on substrates maintained at 100 °C. The evolution of the structure was investigated by infrared-absorption spectrometry, Raman spectrometry and transmission electron microscopy experiments for annealing temperatures less than 600 °C. These experiments allowed us to follow the phase separation of the alloy and to observe the appearance of amorphous and crystallized Ge aggregates. The evolution of the photoluminescence in the range of 560–1550 nm was correlated to the structure of the films.

© 2006 American Institute of Physics. [DOI: 10.1063/1.2218830]

During the last ten years, silicon, germanium, or silicon-germanium quantum dots embedded in an insulator have been studied extensively for their new physical properties induced by the size reduction. They have potential applications for optoelectronic devices or for single-electron devices such as memories. In particular, the optical properties of nanostructures made from silicon or germanium have attracted much attention because it opens new possibilities for optoelectronic applications with group IV elements. Indeed the confinement of carriers in such structures with sizes lower than the exciton Bohr radius leads to a strong enhancement of the radiative transition yield and to the increase of the emitted photons energy.

Silicon nanocrystals can be obtained in substoichiometric SiO_x films prepared by Si implantation in SiO_2 ,^{1,2} plasma enhanced chemical vapor deposition,³ sputtering,⁴ or evaporation.^{5,6} In such silicon suboxides, the silicon clusters are generated by annealing posttreatments which involve in the demixtion of the SiO_x film following the reaction $\text{SiO}_x \rightarrow \text{Si} + \text{SiO}_2$.

Such studies have also been performed to follow the formation of Ge nanocrystals during annealing treatments in SiGeO_x alloys or in GeO_x films prepared by magnetron sputtering,⁷ but there has been very little work done on the PL properties of the Ge nanostructures. In this letter, we report on a study of GeO_x thin films prepared by evaporation of GeO_2 grains. It is shown that annealing treatments enables us to obtain Ge nanocrystals in a GeO_2 matrix. The PL properties are correlated to the evolution of the structure, in particular, to the growth of the nanocrystals.

GeO_2 was evaporated in a high-vacuum chamber from an electron beam gun. The base pressure was 10^{-8} Torr. The pressure during the evaporation increases until 3×10^{-6} Torr. The silicon substrates were maintained at 100 °C. The deposition rate of 0.1 nm/s was controlled by a quartz microbalance. The layer thickness was 200 nm. After deposition, the films were annealed in a high-vacuum quartz tube with a tubular oven. The heating rate was $10^\circ\text{C min}^{-1}$. When the annealing temperature T_a was reached, this oven was pushed away and the films cooled naturally.

The evolution of the atomic structure and of the oxygen bonding configurations was followed by infrared (IR) ab-

sorption spectroscopy, Raman spectroscopy and transmission electron microscopy (TEM) observations. The normal incidence IR absorption measurements were carried out with a resolution of 4 cm^{-1} . The baseline of the spectra was subtracted. Raman measurements were achieved with a multi-channel spectrometer equipped with a 1800 grooves/mm grating. The 488 nm excitation light source was emitted by an argon laser.

Photoluminescence excitation at 355 nm was performed using a frequency-trippled YAG (yttrium aluminum garnet):Nd laser. Optical emission was analyzed by a monochromator equipped with a 600 grooves/mm grating and by a near infrared photomultiplier tube cooled at 190 K. The time resolution of the system is around 10 ns. The response of the detection system was precisely calibrated with a tungsten wire calibration source. For PL measurements, the films were maintained at 77 K.

Figure 1 presents the IR absorption spectra of the samples as-deposited and annealed at different temperatures T_a . Only the range of $400\text{--}1200\text{ cm}^{-1}$ is presented since the Ge–OH bonds are not visible around 3400 cm^{-1} . For the as-deposited sample, two intense Ge–O bands are observed at 524 and 825 cm^{-1} . They are assigned to the Ge–O–Ge bending vibration mode and to the stretching vibration mode of the same group, respectively.⁸ With annealing, the absorption intensity of these Ge–O–Ge bands increases and their frequency shifts towards higher wave numbers (from 524 to 570 cm^{-1} and from 824 to 870 cm^{-1} , respectively). Such a shift has already been observed in substoichiometric SiO_x alloys by several groups^{9,10} which have shown that the

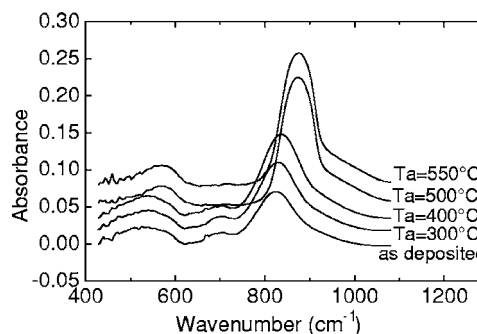


FIG. 1. IR absorption spectra of the GeO_x films annealed at different temperatures T_a .

^{a)}Electronic mail: vergnat@lpm.u-nancy.fr

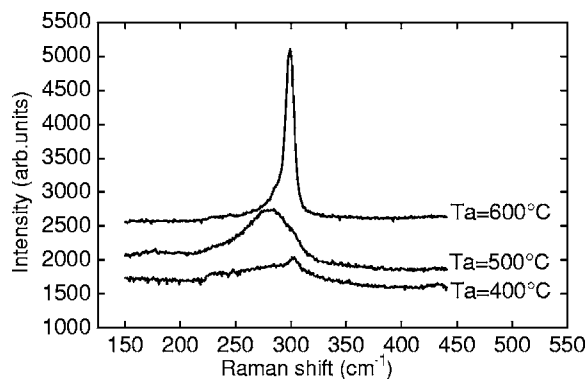


FIG. 2. Raman spectrometry spectra of GeO_x films annealed at different temperatures T_a .

frequency of these peaks increases with the oxygen composition of the films, due to the strong electronegativity of the second-nearest-neighbor oxygen atoms.

Therefore, during evaporation, there is partial decomposition of the GeO_2 source by the electron beam, which explains the increase of the pressure in the chamber, and the deposited films are substoichiometric. Moreover, the shift of the peaks towards higher frequencies shows that the suboxide evolved into the Ge dioxide phase. As the average chemical composition remains unchanged, it can be concluded that a phase separation appears in the film and that pure Ge or Ge-rich areas appear in the samples, following the reaction $\text{GeO}_x \rightarrow \text{Ge} + \text{GeO}_2$. It is difficult to say whether the decomposition is finished for T_a equal to 550 °C, but the measured values of the peaks positions are slightly higher than those obtained for thin films by Lucovsky *et al.*⁸ [560 and 860 cm^{-1} in $a\text{-Ge}:(\text{O}-\text{H})$ alloys prepared by glow discharge of germane with water vapor] and by Busani *et al.*¹¹ (561 and 858 cm^{-1} for an anodic oxide). Moreover, it was not possible to study the structure for annealing temperatures higher than 600 °C. Indeed, for these temperatures, the peaks shift towards lower wave numbers and their intensity decreases because the germanium oxide phase becomes volatile.

Another weak absorption band is visible near 700 cm^{-1} for the as-deposited film and the film annealed at 300 °C. As proposed by Busani *et al.*,¹² this band is probably a stretching mode of dangling GeO bonds. This hypothesis is confirmed by the disappearance of this band for the higher annealing temperatures which generally corresponds to a densification of the atomic structure and the disappearance of the dangling bonds.

Raman spectroscopy is a very efficient method to observe the presence of Ge on its crystalline or amorphous form. Bulk crystalline Ge is characterized by an intense and thin band at 300 cm^{-1} , which corresponds to the transverse optic (TO) mode of phonons. In the case of amorphous Ge, the disorder changes the vibrational density of states and the Raman spectrum¹³ is characterized by a broad band at 270 cm^{-1} .

Figure 2 shows Raman shifts of GeO_x films annealed at different temperatures T_a . For T_a less than 400 °C, the spectrum only shows very weak bands at 300 and 430 cm^{-1} which correspond to the vibrational modes of the crystalline silicon substrate. This means that the films do not contain Ge aggregates. For T_a equal to 500 °C, the spectrum shows the signal of the film, i.e., a broad band at 270 cm^{-1} , corresponding to the presence of an amorphous phase of Ge. For T_a

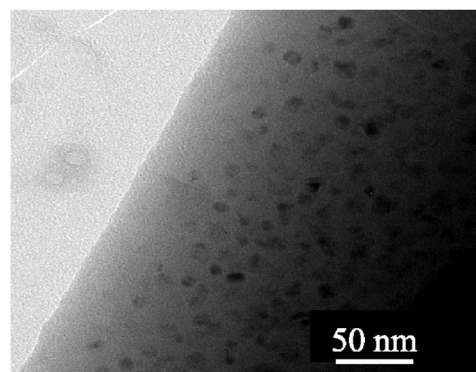


FIG. 3. TEM micrograph of a GeO_x film annealed at 600 °C.

equal to 600 °C, the amorphous peak disappears and a sharp peak appears at 300 cm^{-1} , which corresponds to the formation of crystalline Ge. The peak presents a low-frequency asymmetric broadening, which suggests the presence of nanocrystals.¹⁴ The presence of a crystallized GeO_2 phase, characterized by a Raman shift¹⁵ at 440 cm^{-1} , was not observed.

These results are in agreement with the IR spectrometry results. They strongly suggest that a phase separation process happens in the films to form the two more stable $a\text{-Ge}$ and $a\text{-GeO}_2$ phases. For T_a equal to 600 °C, the Ge phase is crystallized but the GeO_2 phase remains amorphous.

TEM micrographs confirm these results. Whereas the samples annealed at 500 °C show micrographs and diffraction patterns typical of an amorphous phase, the micrographs of the samples annealed at 600 °C show nanocrystals with sizes of a few nanometers (Fig. 3) and their diffraction patterns show the diffraction lines corresponding to crystalline Ge.

Figure 4 presents PL spectra of GeO_x films annealed at different temperatures T_a . For the films as-deposited and annealed at 300 and 350 °C, the PL spectra show a very broad band between 560 and 1550 nm, with an intense and narrow band near 1000 nm. The typical decay time of these bands are below 20 ns. As these bands are proportional, they must have the same origin. Their intensity slightly increases with T_a until 350 °C. For T_a equal to 400 and 450 °C, these bands disappear and another weaker and broad band appears with a maximum near 1250 nm and with a typical decay time equal to 200 ns. This band redshifts near 1400 nm for T_a

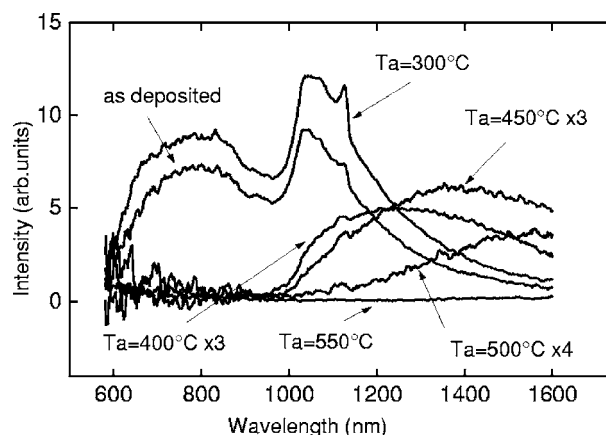


FIG. 4. PL spectra of GeO_x films annealed at different temperatures T_a .

equal to 500 °C and there is no more PL for T_a equal to 550 °C.

To understand the origin of these bands, it must be to recall that the PL of Si nanocrystals has mainly two components: a “blue” one generally associated with defects in the surrounding oxide and a “red” one coming either from the recombination of electron-hole pairs in nanocrystals or from the trapping on a surface defect.¹⁶ In comparison to silicon, there has been little work done on Ge nanostructures and PL has been observed mainly in Ge nanocrystals embedded in SiO₂ matrices. There are several reports of a “blue-green” PL with a maximum below 620 nm independently of the size of the nanocrystals.¹⁷ For example, Kartopu *et al.*¹⁸ have observed, in a spark-processed Ge, a broad “orange” band between 520 and 820 nm attributed to defects in the GeO_x phase. But recently, Takeoka *et al.*¹⁹ have observed a size-dependent PL in the near-infrared region which is closer to the band gap of bulk Ge and which is more compatible with the quantum confinement model.

The broad band observed in our samples as-deposited and annealed at 300 and 350 °C is rather similar to the bands generally attributed to the defects in the oxide phase. With annealing at temperatures higher than 400 °C, IR absorption experiments have shown that there is a strong modification of the structure, characterized by an important shift of the stretching vibration band and by the disappearance of the 700 cm⁻¹ band attributed to defects. This last result is in agreement with the suppression of this broad PL band for T_a equal to 400 °C. Moreover, the fast PL decay time of this band is typical of defects luminescence.

After this structural modification, it remains (or it appears) a weak band with a maximum near 1240 nm for T_a equal to 400 °C. This band redshifts with increasing T_a with energy slightly higher than the band gap of Ge. Its observation corresponds to the phase separation of the alloys and to the appearance of the amorphous Ge aggregates, as shown by the IR absorption and Raman spectrometry experiments. Its redshift with increasing T_a and therefore with increasing aggregates size is in agreement with the quantum-confinement theory. Moreover, the measured PL decay time of this band is in agreement with the lifetimes values predicted by Niquet *et al.*¹⁷ for Ge nanocrystals. This PL band could then be attributed to the Ge aggregates.

In conclusion, visible and near-infrared PLs can be observed in GeO_x films prepared by evaporation of GeO₂ powder from an electron beam gun. With thermal annealing, the films present a phase separation inducing the appearance of Ge aggregates in a GeO₂ matrix. The evolution of the IR absorption and Raman spectrometries correlated to the PL experiments suggests that the PL originates in the presence of defects in the oxide matrix for annealing temperatures less than 350 °C and in the Ge aggregates for higher annealing temperatures.

The authors wish to acknowledge F. Mouginet and J. Arocas-Garcia for the sample preparation.

¹T. Shimizu-Iwayama, K. Fujita, S. Nakao, K. Saitoh, T. Fujita, and N. Itoh, *J. Appl. Phys.* **75**, 7779 (1994).

²J. G. Zhu, C. W. White, J. D. Budai, S. P. Withrow, and Y. Chen, *J. Appl. Phys.* **78**, 4386 (1995).

³A. J. Kenyon, P. F. Trwoga, C. W. Pitt, and G. Rehm, *J. Appl. Phys.* **79**, 9291 (1996).

⁴S. Charvet, R. Madelon, F. Gourbilleau, and R. Rizk, *J. Appl. Phys.* **85**, 4032 (1999).

⁵H. Rinnert, M. Vergnat, G. Marchal, and A. Burneau, *Appl. Phys. Lett.* **72**, 3157 (1998).

⁶M. Molinari, H. Rinnert, and M. Vergnat, *Appl. Phys. Lett.* **82**, 3877 (2003).

⁷M. Zacharias, J. Bläsing, M. Löhmman, and J. Christen, *Thin Solid Films* **278**, 32 (1996).

⁸G. Lucovsky, S. S. Chao, J. Yang, J. E. Tyler, R. C. Ross, and W. Czubatyj, *Phys. Rev. B* **31**, 2190 (1985).

⁹P. G. Pai, S. S. Chao, Y. Takagi, and G. Lucovsky, *J. Vac. Sci. Technol. A* **4**, 689 (1986).

¹⁰H. Rinnert, M. Vergnat, and A. Burneau, *J. Appl. Phys.* **89**, 237 (2001).

¹¹T. Busani, H. Plantier, R. A. B. Devine, C. Hernandez, and Y. Campidelli, *J. Non-Cryst. Solids* **254**, 80 (1999).

¹²T. Busani, H. Plantier, R. A. B. Devine, C. Hernandez, and Y. Campidelli, *J. Appl. Phys.* **85**, 4262 (1999).

¹³G. V. M. Williams, A. Bittar, and H. J. Trodahl, *J. Appl. Phys.* **67**, 1874 (1990).

¹⁴J. Gonzalez-Hernandez, G. H. Azerbayejani, R. Tsu, and F. H. Pollak, *Appl. Phys. Lett.* **47**, 1350 (1985).

¹⁵J. H. Chen, D. Pang, H. M. Cheong, P. Wickbolt, and W. Paul, *Appl. Phys. Lett.* **67**, 2182 (1995).

¹⁶M. V. Wolkin, J. Jorne, P. M. Fauchet, G. Allan, and C. Delerue, *Phys. Rev. Lett.* **82**, 197 (1999).

¹⁷Y. M. Niquet, G. Allan, C. Delerue, and M. Lanno, *Appl. Phys. Lett.* **77**, 1182 (2000).

¹⁸G. Kartopu, S. C. Bayliss, R. E. Hummel, and Y. Ekinici, *J. Appl. Phys.* **95**, 3466 (2004).

¹⁹S. Takeoka, M. Fujii, S. Hayashi, and K. Yamamoto, *Phys. Rev. B* **58**, 7921 (1998).